NRC Publications Archive
Archives des publications du CNRC

Higher-order structure of barley chromosomes observed by electron tomography

Hayashida, Misa; Sartsanga, Channarong; Phengchat, Rinyaporn; Malac, Marek; Harada, Ken; Akashi, Tetsuya; Fukui, Kiichi; Ohmido, Nobuko

This publication could be one of several versions: author’s original, accepted manuscript or the publisher’s version. / La version de cette publication peut être l’une des suivantes : la version prépublication de l’auteur, la version acceptée du manuscrit ou la version de l’éditeur.
For the publisher’s version, please access the DOI link below./ Pour consulter la version de l’éditeur, utilisez le lien DOI ci-dessous.

Publisher’s version / Version de l'éditeur:
https://doi.org/10.1016/j.micron.2022.103328
Micron, 160, C, 2022-07-14

NRC Publications Archive Record / Notice des Archives des publications du CNRC :
https://nrc-publications.canada.ca/eng/view/object/?id=a5e483d6-5618-4fa1-ad50-eba8b74f3944
https://publications-cnrc.canada.ca/fra/voir/objet/?id=a5e483d6-5618-4fa1-ad50-eba8b74f3944

Access and use of this website and the material on it are subject to the Terms and Conditions set forth at
https://nrc-publications.canada.ca/eng/copyright
READ THESE TERMS AND CONDITIONS CAREFULLY BEFORE USING THIS WEBSITE.

L’accès à ce site Web et l’utilisation de son contenu sont assujettis aux conditions présentées dans le site
https://publications-cnrc.canada.ca/fra/droits
LISEZ CES CONDITIONS ATTENTIVEMENT AVANT D’UTILISER CE SITE WEB.

Questions? Contact the NRC Publications Archive team at PublicationsArchive-ArchivesPublications@nrc-cnrc.gc.ca. If you wish to email the authors directly, please see the first page of the publication for their contact information.

Vous avez des questions? Nous pouvons vous aider. Pour communiquer directement avec un auteur, consultez la première page de la revue dans laquelle son article a été publié afin de trouver ses coordonnées. Si vous n’arrivez pas à les repérer, communiquez avec nous à PublicationsArchive-ArchivesPublications@nrc-cnrc.gc.ca.

National Research Council Canada
Conseil national de recherches Canada

Submitted to Micron special issue

Higher-order structure of barley chromosomes observed by electron tomography.

Misa Hayashida[1*], Channarong Sartsanga[2], Rinyaporn Phengchat[2], Marek Malac[1,3], Ken Harada[4], Tetsuya Akashi[5], Kiichi Fukui[6], Nobuko Ohmido[2]

[1] Nanotechnology Research Centre, National Research of Council, 11421 Saskatchewan Drive, T6G 2M9, Edmonton, Alberta, Canada.
[2] Graduate School of Human Development and Environment, Kobe University, Tsurukabuto 3-11, Nada-ku, 657-8501, Kobe, Japan.
[3] Department of Physics, University of Alberta, Edmonton, Alberta T6G 2E1, Canada.
[4] Center for Emergent Matter Science (CEMS), RIKEN, Hatoyama, Saitama 350-0395, Japan.
[5] Research & Development Group, Hitachi, Ltd., Hatoyama, Saitama 350-0395, Japan.
[6] Graduate School of Pharmaceutical Sciences, Osaka University, Yamadaoka 1-6, Suita 565-0871, Osaka, Japan
*misa.hayashida@nrc-cnrc.gc.ca

Abstract

The higher order structure of the metaphase chromosome has been an enigma for over a century and several different models have been presented based on results obtained by a variety of techniques. Some disagreements in the results between methods have possibly arisen from artifacts caused during sample preparation such as staining and dehydration. Therefore, we treated barley chromosomes with ionic liquid to minimize the effects of dehydration. We also observed chromosomes on a film with holes to keep pristine chromosome structure from being flattened as seen when placed on a continuous support film. A chromosome placed over a hole in a thin carbon film was mounted on a tomography holder, and its structure was observed in three dimensions (3D) using electron tomography. We found that there are periodic structures with 300-400 nm pitch along the axis in barley chromosomes. The pitch sizes are larger than those observed in human chromosomes.

1. Introduction

Since the discovery of chromosomes in the mid-19th century there have been sustained research efforts to elucidate their structure. Comprehensive chromosome structure, however, has remained an enigma and the detailed internal structure is still controversial.

The Hi-C method (Lieberman-Aiden et al., 2009) has been used to detect the interaction of each position of chromatin fibers as a means to understand the internal structure of chromosomes for the past 10 years. The Hi-C contact matrix of metaphase human chromosomes with polymer simulations showed that metaphase Hi-C data are inconsistent with classic hierarchical models and are instead best described by a linearly organized longitudinally compressed array of consecutive chromatin loops (Naumova et al., 2013).

The Hi-C method (Belton et al., 2012) was also utilized for chicken (Gibcus et al., 2018), giant axolotl (Schloissnig et al., 2021) and barley (Kubalová et al., 2021) chromosomes. Gibcus et al. (2018) found that chicken chromosomes in prometaphase adopt a spiral staircase-like structure with a helically arranged axial scaffold of condensin II at the bases of chromatin loops by polymer simulations of Hi-C data. They estimated the height of one helical turn to be ~200 nm, which is consistent with microscope observations suggesting that consecutive genomic loci follow a helical gyre with a pitch of ~250 nm within the cylindrical shape of chromatids (Strukov and Belmont, 2009; Strukov et al., 2003). Schloissnig et al. (2021) found that in axolotl mitotic chromosomes, a 35 Mb helical turn is predicted, which is threefold longer than chicken chromosomes in Gibcus et al. (2018). From a combination of barley metaphase chromosome-derived Hi-C data, oligo-FISH, sister chromatid exchange detection, super-resolution microscopy, and polymer simulation, Kubalová et al. (2021) concluded that sister chromatids are formed by chromatin helices of identical handedness. The helical turns span 20-38 Mb creating a ~400 nm thick fiber.

Imaging techniques such as transmission electron microscopy (TEM), scanning electron microscopy (SEM) and atomic force microscopy (AFM) can be utilized to confirm the results. Helical structures have been observed in TEM and SEM since the 1970s. Helical turns were observed in chromosomes of animals such as frogs (Seto, 1972) and humans (Boy de la Tour and Laemmli, 1988; Ohnuki, 1968; Rattner and Lin, 1985; Sumner, 1991; Ushiki et al., 2002; Utsumi, 1982). Helical turns of 450-550 nm chromatin fibers were also observed in onions (Hao et al., 1990; 1988).

We previously visualized longitudinally compressed stacks with 100–200 nm periodicity along the chromosome axis in an isolated human chromosome (Hayashida et al., 2021). The observed shapes are closer to parallel decks rather than helixes. The structures are longitudinal, but not axial. Similar images were presented in Fig. 7 in Rattner and Lin (1985), Figs. 2 and 7 in (Ushiki et al., 2002) and Fig. 1 in Strukov and Belmont (2009). It is also consistent with the Hi-C data of metaphase human chromosomes (Naumova et al., 2013). If the compressed stacks were part of helical shapes, the boundaries between the stacks would be tilted from the direction perpendicular to the chromosome axis. Whether chromosome higher-order structure is longitudinal or axial might depend on the cell cycle stage, or their origins (species of animals or plants etc.). Further investigation will be necessary to fully understand the internal structure of chromosomes.

Although structures with size exceeding 100 nm were observed by TEM, AFM, SEM and Hi-C as we summarized in the previous two sections, periodic structure larger than 11 nm was not detected in human chromosomes by cryo-EM (Eltsov et al., 2008; Maeshima et al., 2010). The chromosomes were not treated with any staining or chemical fixation while most chromosomes mentioned in the last two paragraphs were stained and fixed with chemicals. However, the thickness of sections observed by cryo-EM is typically about 40 nm. Therefore, it is unlikely that structures larger than 40 nm would be recognized in such sections. In other words, these results might not confirm that staining and chemical fixation generate structures larger than 100 nm.

In this paper, we observed barley by electron tomography (ET) and compared the results to human chromosomes (Hayashida et al., 2021) to investigate differences and similarities between human chromosomes and barley chromosomes. We observed OsO_4 -stained chromosomes placed on a continuous thin carbon film. We also observed unstained chromosomes on a thin carbon film with holes to prevent chromosomes from being flattened at the carbon-chromosome interface, for example by surface tension (Hayashida et al., 2015; Hayashida and Malac, 2017). We detected the presence of similar longitudinally compressed stacks in human and barley chromosomes. The pitch of the stacks is 300-400 nm along the chromosome axis.

2. Materials and Methods

Barley chromosomes were isolated and purified as described in the previous paper (Sartsanga et al., 2021). Barley chromosomes stained with OsO_4 were prepared by the ChromEM procedure (Ou et al., 2017). In brief, the buffer solution containing the chromosomes was then dropped onto carbon/formvar support film on a grid for TEM. Chromosomes were fixed with 2.5% (v/v) glutaraldehyde in 0.1 M Na-cacodylate, 5 mM $CaCl_2$, pH 7.4, at 4˚C overnight. Fixed chromosomes were washed five times for two minutes in 0.1 M sodium cacodylate buffer and treated for 15 minutes with blocking buffer (10 mM potassium cyanide in 0.1 M sodium cacodylate). DNA was stained with DRAQ5 (10 μM) in 0.1% saponin, 0.1 M cacodylate buffer for 10 minutes followed by washing with the blocking buffer three times for five minutes. The grid was transferred to a glass-bottom dish contained 2.5 mM diaminobenzidine tetrahydrochloride (DAB) in 0.1 M sodium cacodylate buffer and placed under the fluorescence microscope. For DAB photo-oxidation, chromosomes on the grid were continuously fluorescence illuminated under Cy5 channels for 30 minutes then rinsed five times for two minutes with 0.1 M sodium cacodylate buffer. Chromosomes were then stained for 30 minutes with 2% OsO_4in 0.15 M sodium cacodylate buffer, 2 mM $CaCl_2$, 1.5% potassium ferrocyanide followed by washing with distilled water five times for two minutes. For TEM observation, chromosomes were treated with 0.5% ionic liquid (IL) butyl-methyl-imidazolium tetrafluoroborate ($BMI\text{-}BF_4$) (TCI, Japan) for 1 min and dried in a vacuum pumping system for 2 h. The chromosomes were transferred from the support film and transferred to a 360˚ rotation holder (Tanigaki et al., 2015; Tsuneta et al., 2014) in a focused ion beam instrument using the method described in our previous paper (Phengchat et al., 2019).

Unstained barley chromosomes were prepared by following the procedure in previous paper (Sartsanga et al., 2021). The buffer solution containing the chromosomes was dropped onto QUANTIFOIL® Holey Carbon Films on a grid. The film has 3 μm diameter prefabricated holes. The holes prevent excessive ionic liquid from remaining on the surface of chromosomes and also prevent chromosome from being flattened at the carbon-chromosome interface in the areas where chromosome is suspended over the holes. Chromosomes were fixed with 2.5% (v/v) glutaraldehyde in PBS at 4°C overnight then washed three times with PBS for 5 minutes each. After fixation, chromosomes were treated with 0.5% $BMI\text{-}BF_4$ and dried as described above. A chromosome which makes a bridge over a hole was transferred to a 360˚ rotation holder (Yaguchi et al., 2008). The QUANTIFOIL® Holey Carbon Film has holes and it is not sufficiently strong to hold chromosomes for the acquisition duration of a tomography tilt series. Therefore, carbon frame was deposited on the left and right sides (as we describe later) in FIB to prevent the film from bending.

A stained barley chromosome was observed in a Hitachi 1 MV Field Emission (FE) TEM (Kawasaki et al., 2000a; Kawasaki et al., 2000b). Unstained barley chromosomes were observed in a Hitachi H9500 TEM operated at 300 kV acceleration voltage. A tomography series consisting of 61 images was collected with a 3° tilt step (Hayashida and Malac, 2016; Hayashida et al., 2018) over the entire 0° to 180° tilt range in both microscopes. The image sizes for the 1 MV-TEM were 3710×3838 pixels with a 1.77 nm pixel size in a Gatan direct exposure K2 camera, and 1336 x 2004 pixels with a 5.2 nm pixel in a Gatan Ultrascan 1000™ slow scan CCD camera in the Hitachi H9500. Composer and Visualizer by TEMography.com, were used for reconstruction of all the tilt series and visualization of the tomograms.

3. Results

3.1 OsO_4 stained barley chromosome on a continuous carbon film

Isolated barley chromosomes with OsO_4 -labelled DNA molecules were observed with ET. The chromosomes were placed on a continuous carbon film. Figs. 1a, b and c show a TEM image observed using 1 MV-TEM, a tomogram, and one of the slices extracted from the tomogram near the top surface of the chromosome. Here, we note that TEM images are a sum of the intensity along the beam direction. In thick samples, as used here, TEM images further suffer from the "top-bottom" effect (Reimer and Kohl, 2008). Tomograms differ from TEM images by providing the 3D volume of the sample without integration along the beam path, resulting in isotropic resolution in 3D. Slices extracted from tomograms display more internal structures than tomograms and tomograms can display more detailed sample surface morphology than TEM images. Although there is no visible structure in the TEM image and the tomogram, we can observe the longitudinally compressed stacks along the chromosome in the *slice image* extracted from the tomogram, as shown in Fig. 1c. The area bordered by the solid line in Fig. 1c shows features with a 300-400 nm period within the chromosome in the line profile (Fig. 1d). The longitudinally compressed stacks along the chromosome axis are very similar to the slice image observed in a human chromosome (Hayashida et al., 2021) except for the pitch. As reported in the previous paper (Hayashida et al., 2021), the stacks were not observed near the carbon support film but rather near the top surface of the barley chromosomes because the bottom side of the chromosome is flattened to maximize its contact with the support film in order to reduce its surface energy (Hayashida et al., 2015).

3.2 Unstained barley chromosome suspended over holes in a thin carbon film

Fig. 2a shows a TEM image observed using 300 kV-TEM of an unstained barley chromosome on a thin carbon film with holes. Additional carbon (that looks like a picture frame) was deposited using a focused ion beam on the carbon film on both the left and right sides of the chromosome to make the sample support sturdier for data acquisition as shown in the dashed rectangles in Fig. 2a. A contrast-adjusted image is shown in Fig. 2b and the longitudinally compressed stacks with 300-400 nm pitch (bordered in yellow) are observed. The stacks are not visible in the tomogram, so the tomogram is not included here. It is possible that the sample surface has residual ionic liquid making it difficult to observe the surface structure of the chromosome. Here, we note that the chromosome is not stained and the image intensity arising from the chromosome alone in TEM is almost the same as ionic liquid or buffer.

Conversely, a barley chromosome in Figs. 3 and 4 where carbon film with holes was also used to support the chromosome shows stacks clearly not only in a TEM image, but also in the tomogram. Additional carbon frame was also deposited on both the left and right sides of the chromosome using a focused ion beam. The line profiles from the chromosome in Fig. 3b show that there are longitudinally compressed stacks with 300-400 nm pitch along the chromosome axis. Fig. 4a shows a tomogram of the chromosome in Fig. 3a. The longitudinally compressed stacks (particularly along the chromosome axis) on the surfaces from both front and back (film) sides can be partially seen in Fig. 3a. The boundaries of the stacks are traced with yellow lines in Fig. 4b for clarity. The stacks' positions at the front and back sides' images exhibit mirror symmetry. This means that the stacks are observed at the same positions in the front and back side of the chromosome. Low contrast may explain why the stacks were only partially observed as shown in Fig. 3 because the chromosome was not stained.

4. Discussion

We observed longitudinally compressed stacks along the barley chromosome axes which were similar to the structures we observed in human chromosomes. ("Structure A" in Hayashida et al., 2021). While the periodicity of the stacks was 100-200 nm for human chromosomes, 300-400 nm was observed in barley chromosomes in this paper.

When isolated chromosomes are dried on a film, the bottom part is flattened because of adhesion. Similar adhesion happens on polystyrene latex nanoparticles (Hayashida et al., 2015; Hayashida and

Malac, 2017). Therefore, stacks are observed only on the top surface in human chromosomes (Hayashida et al., 2021; Rattner and Lin, 1985; Ushiki et al., 2002; Strukov and Belmont, 2009). It may have been suspected that the stacks arise during the chromosomes' drying. However, our results deny this suspicion because we could eliminate the interaction by suspending chromosomes over a carbon thin film with holes. Moreover, stacks were observed on the surface of an unstained chromosome for the first time. In our previous paper (Hayashida et al., 2021), we could not observe the stacks in unstained chromosomes on a continuous film in TEM images although the stacks of the chromosomes were observed in electron diffraction patterns. It is possible that the holes in the thin carbon film we used this time prevented excessive ionic liquid from remaining on the surface of chromosomes and the chromosome surface structure became more visible as a result as shown in Fig. 2-4.

Our results showed that the positions of stacks were the same on both the top (opposite the film side) and the film side. If the structures were helical, the positions would follow helical patterns, and the stacks would be tilted from the direction perpendicular to the chromosome axis. Our results appear to be consistent with the model for human chromosomes (Borland et al., 1988) in which DNA fiber loops are randomly oriented within regions of roughly 200 nm axial extent along the long axis of each chromatid and adjacent regions may slightly overlap with each other. The periodic features are longitudinal, but not axial as suggested in Naumova et al. (2013). Similar images, in which the stacks were aligned along the chromosome axis, were presented in Fig. 7 in Rattner and Lin (1985), Figs. 2 and 7 in Ushiki et al. (2002) and Fig. 1 in Strukov and Belmont (2009).

It is still unknown why axial helix shapes were observed in some cases and longitudinally compressed stacks were observed in others including this paper. The shape may be changed between helical and longitudinally compressed stacks during isolation, drying or during the cell cycle. What can be concluded is that barley chromosomes exhibit 300-400 nm periodic stacks (vs. 100-200 nm in humans) along the chromosome long axis. This periodicity was also confirmed by the Hi-C technique (Kubalová et al., 2021; Naumova et al., 2013).

In the Borland et al. (1988) model, the 200 nm region consists of 30 nm fibers Sartsanga et al. (2021) found barley chromosome chromatin fibers 11.6 ± 3.5 nm on the chromosome surface. On the other hand, 80 nm chromatin fibers without large cavities were observed in Kubalová et al. (2021). However, we did not observe 30 nm or 80 nm structures in human and barley chromosomes, probably due to the dense packing of fibers in the chromosomes. Further investigation is necessary to elucidate chromosome higher-order structures.

5. Conclusion

We observed stained chromosomes placed on a continuous thin carbon film and unstained chromosomes on a thin carbon film with holes by ET. We detected the presence of similar longitudinally compressed stacks in both the stained and unstained barley chromosomes. The pitch of the stacks is 300-400 nm along the chromosome axis. The holes in the thin carbon film prevented excessive ionic liquid from remaining on the surface of chromosomes and the chromosome surface structure on both the top (opposite to the film) side and the bottom (film) side became more visible as a result.

Acknowledgments

This work was supported by the Japan Science and Technology Agency (JST) SICORP (17935614, 2017–2022) to Kiichi Fukui and the Mitsubishi Foundation: 202010011 to Nobuko Ohmido.

Figure captions

Figure 1
(a) A TEM image observed using a 1MV-TEM of an isolated barley chromosome whose DNA molecules were labelled with OsO_4. The chromosome is placed on a continuous carbon film.
(b) A tomogram of the chromosome.
(c) A slice image of the tomogram in (b)
(d) A line profile from inside the white line from top to bottom in (c).

Figure 2
(a) A TEM image observed using a 300kV-TEM of an unstained barley chromosome on a film with holes.
(b) A contrast enhanced image of (a).
(c) Boundaries of the stacks in (b) are traced with yellow lines.

Figure 3
(a) A TEM image observed using a 300kV-TEM of an unstained barley chromosome on a film with holes.
(b) Line profiles from inside the white lines in (a).

Figure 4
(a) Tomograms of the unstained barley chromosome shown in Fig. 3 from front and back (film) sides.

(b) Stack boundaries were traced with yellow lines.

References

Belton, J.M., McCord, R.P., Gibcus, J.H., Naumova, N., Zhan, Y., Dekker, J., 2012. Hi-C: a comprehensive technique to capture the conformation of genomes. Methods 58, 268-276.

Borland, L., Harauz, G., Bahr, G., Heel, M.v., 1988. Packing of the 30 nm chromatin fiber in the human metaphase chromosome. Chromosoma 97, 159-163.

Boy de la Tour, E., Laemmli, U.K., 1988. The metaphase scaffold is helically folded: sister chromatids have predominantly opposite helical handedness. Cell 55, 937-944.

Eltsov, M., MacLellan, K.M., Maeshima, K., Frangakis, A.S., Dubochet, J., 2008. Analysis of cryo-electron microscopy images does not support the existence of 30-nm chromatin fibers in mitotic chromosomes in situ. PNAS 105, 19732–19737.

Gibcus, J.H., Samejima, K., Goloborodko, A., Samejima, I., Naumova, N., Nuebler, J., Kanemaki, M.T., Xie, L., Paulson, J.R., Earnshaw, W.C., Mirny, L.A., Dekker, J., 2018. A pathway for mitotic chromosome formation. Science 359.

Hao, S., Jiao, M., Huang, B., 1990. Chromosome organization revealed upon the decondensation of telophase chromosomes in Allium. CHROMOSOMA 99, 371-378.

Hao, S., Xing, M., Jiao, M., 1988. Chromatin-free compartments and their contents in anaphase chromosomes of higher plants. Cell Biology International Reports 12, 627-634.

Hayashida, M., Kumagai, K., Malac, M., 2015. Three dimensional accurate morphology measurements of polystyrene standard particles on silicon substrate by electron tomography. Micron 79, 53-58.

Hayashida, M., Malac, M., 2016. Practical electron tomography guide: Recent progress and future opportunities. Micron 91, 49-74.

Hayashida, M., Malac, M., 2017. Sample preparation method for 3D size measurements of polystyrene nanoparticles with nominal 30, 50, 70 and 100 nm diameters by electron tomography. Measurement Science and Technology 28.

Hayashida, M., Ogawa, S., Malac, M., 2018. Evaluation of electron tomography reconstruction methods for interface roughness measurement. Microscopy Research Technique 81, 515-519.

Hayashida, M., Phengchat, R., Malac, M., Harada, K., Akashi, T., Ohmido, N., Fukui, K., 2021. Higher-Order Structure of Human Chromosomes Observed by Electron Diffraction and Electron Tomography. Microsc Microanal 27, 149-155.

Kawasaki, T., Matsui, I., Yoshida, T., Katsuta, T., Hayashi, S., Onai, T., Furutsu, T., Myochin, K., Numata, M., Mogaki, H., Gorai, M., Akashi, T., Kamimura, O., Matsuda, T., Osakabe, N., Tonomura, A., Kitazawa, K., 2000a. Development of a 1 MV field-emission transmission electron microscope. J. Electron Microsc. 6, 711-718.

Kawasaki, T., Yoshida, T., Matsuda, T., Osakabe, N., Tonomura, A., 2000b. Fine crystal lattice fringes observed using a transmission electron microscope with 1 MeV coherent electron waves. Appl. Phys. Lett. 76, 1342-1344.

Kubalová, I., Câmara, A.S., Cápal, P., Beseda, T., Rouillard, J.-M., Krause, G.M., Toegelová, H., Himmelbach, A., Stein, N., Houben, A., Doležel, J., Mascher, M., Šimková, H., Schubert, V., 2021. Helical metaphase chromatid coiling is conserved. bioRxiv.

Lieberman-Aiden, E., van Berkum, N.L., Williams, L., Imakaev, M., Ragoczy, T., Telling, A., Amit, I., Lajoie, B.R., Sabo, P.J., Dorschner, M.O., Sandstrom, R., Bernstein, B., Bender, M.A., Groudine, M., Gnirke, A., Stamatoyannopoulos, J., Mirny, L.A., Lander, E.S., Dekker, J., 2009. Comprehensive mapping of long-range interactions reveals folding principles of the human genome. Science 326, 289-293.

Maeshima, K., Hihara, S., Eltsov, M., 2010. Chromatin structure: does the 30-nm fibre exist in vivo? Curr Opin Cell Biol 22, 291-297.

Naumova, N., Imakaev, M., Fudenberg, G., Zhan, Y., Lajoie, B.R., Mirny, L.A., Dekker, J., 2013. Organization of the Mitotic Chromosome. Science 342, 948-953.

Nishino, Y., Eltsov, M., Joti, Y., Ito, K., Takata, H., Takahashi, Y., Hihara, S., Frangakis, A.S., Imamoto, N., Ishikawa, T., Maeshima, K., 2012. Human mitotic chromosomes consist predominantly of irregularly folded nucleosome fibres without a 30-nm chromatin structure. EMBO J 31, 1644-1653.

Ohnuki, Y., 1968. Structure of chromosomes I. Morphological studies of the spiral structure of human somatic chromosomes. Chromosoma, 402–428.

Ou, H.D., Phan, S., Deerinck, T.J., Thor, A., Ellisman, M.H., O'Shea, C.C., 2017. ChromEMT: Visualizing 3D chromatin structure and compaction in interphase and mitotic cells. Science 357.

Phengchat, R., Hayashida, M., Ohmido, N., Homeniuk, D., Fukui, K., 2019. 3D observation of chromosome scaffold structure using a 360 degrees electron tomography sample holder. Micron 126, 102736.

Rattner, J.B., Lin, C.C., 1985. Radial loops and helical coils coexist in metaphase chromosomes. Cell 42, 291-296.

Reimer, L., Kohl, H., 2008. Transmission Electron Microscopy. Springer-Verlag New York.

Sartsanga, C., Phengchat, R., Fukui, K., Wako, T., Ohmido, N., 2021. Surface structures consisting of chromatin fibers in isolated barley (Hordeum vulgare) chromosomes revealed by helium ion microscopy. Chromosome Res 29, 81-94.

Schloissnig, S., Kawaguchi, A., Nowoshilow, S., Falcon, F., Otsuki, L., Tardivo, P., Timoshevskaya, N., Keinath, M.C., Smith, J.J., Voss, S.R., Tanaka, E.M., 2021. The giant axolotl genome uncovers the evolution, scaling, and transcriptional control of complex gene loci. Proc Natl Acad Sci U S A 118.

Seto, T., 1972. The spiral structure of amphibian somatic chromosomes as observed with a light microscope. . Mem. Fac. Educ., Shimane Univ. (Nat. Sci.), 99-104.

Strukov, Y.G., Belmont, A.S., 2009. Mitotic chromosome structure: reproducibility of folding and symmetry between sister chromatids. Biophys. J. 96, 1617-1628.

Strukov, Y.G., Wang, Y., Belmont, A.S., 2003. Engineered chromosome regions with altered sequence composition demonstrate hierarchical large-scale folding within metaphase chromosomes. J Cell Biol 162, 23-35.

Sumner, A.T., 1991. Scanning electron microscopy of mammalian chromosomes from prophase to telophase. Chromosoma 100, 410-418.

Tanigaki, T., Takahashi, Y., Shimakura, T., Akashi, T., Tsuneta, R., Sugawara, A., Shindo, D., 2015. Three-dimensional observation of magnetic vortex cores in stacked ferromagnetic discs. Nano Lett 15, 1309-1314.

Tsuneta, R., Kashima, H., Iwane, T., Harada, K., Koguchi, M., 2014. Dual-axis 360 degrees rotation specimen holder for analysis of three-dimensional magnetic structures. Microscopy 63, 469-473.

Ushiki, T., Hoshi, O., Iwai, K.I., Kimura, E., Shigeno, M., 2002. The structure of human metaphase chromosomes: its histological perspective and new horizons by atomic force microscopy. Arch. Histol. Cytol. 65, 377-390.

Utsumi, K.R., 1982. Scanning electron microscopy of Giemsa-stained chromosomes and surface-spread chromosomes. Chromosoma 86, 683-702.

Yaguchi, T., Konno, M., Kamino, T., Watanabe, M., 2008. Observation of three-dimensional elemental distributions of a Si device using a 360 degrees -tilt FIB and the cold field-emission STEM system. Ultramicroscopy 108, 1603-1615.

Fig. 1

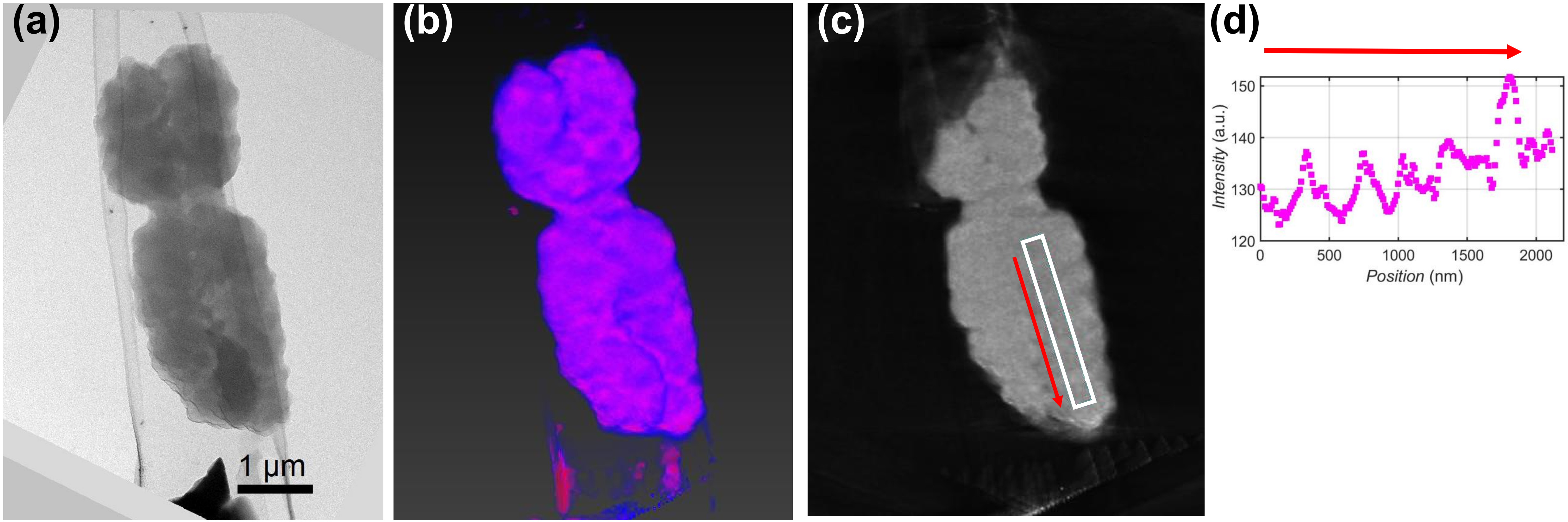
(a)
1 μm
(b)
(c)
(d)
150
140
130
120
Intensity (a.u.)
0
500
1000
1500
2000
Position (nm)

Fig. 2

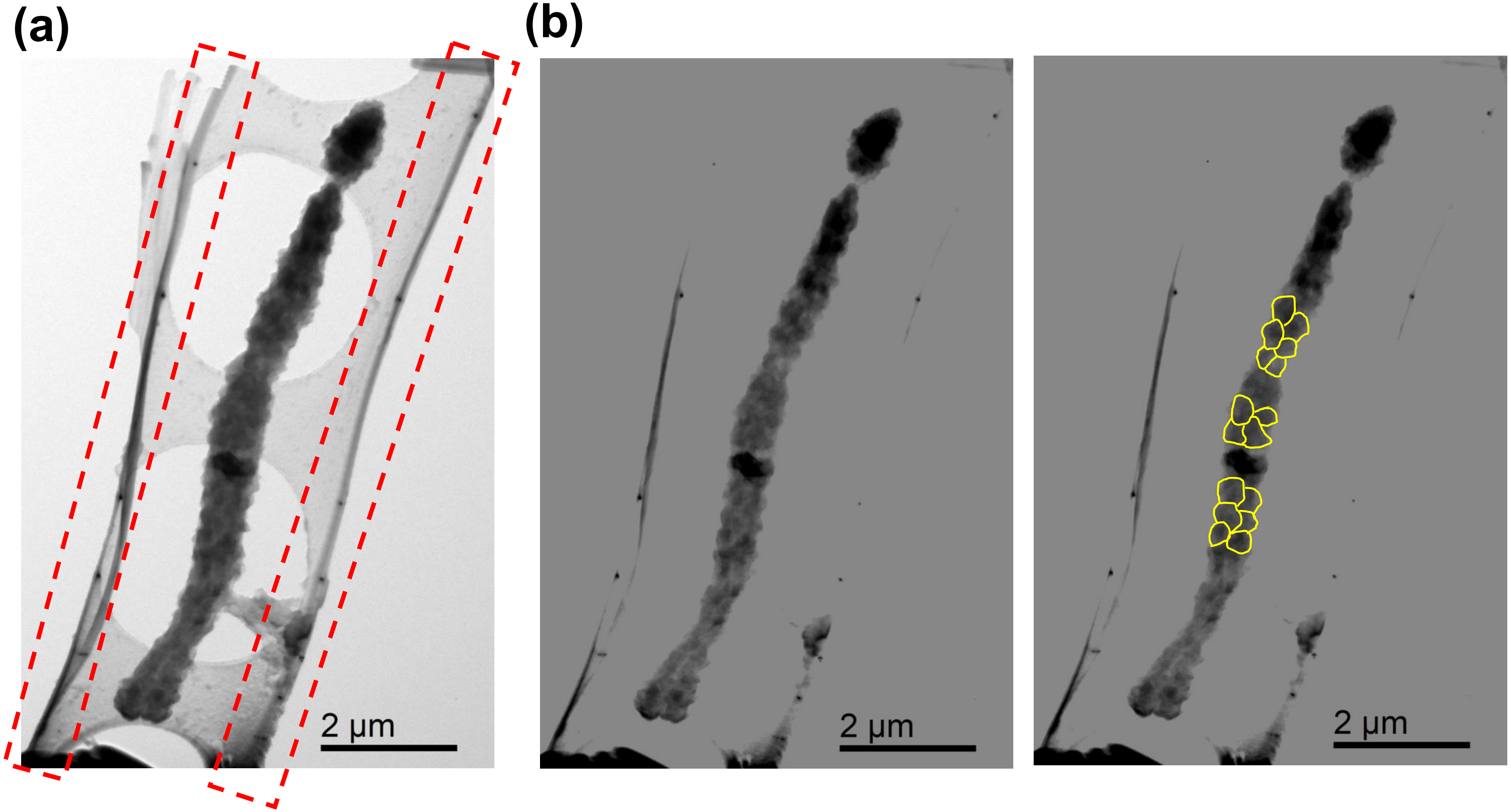

Original

Contrast adjusted

Fig. 3

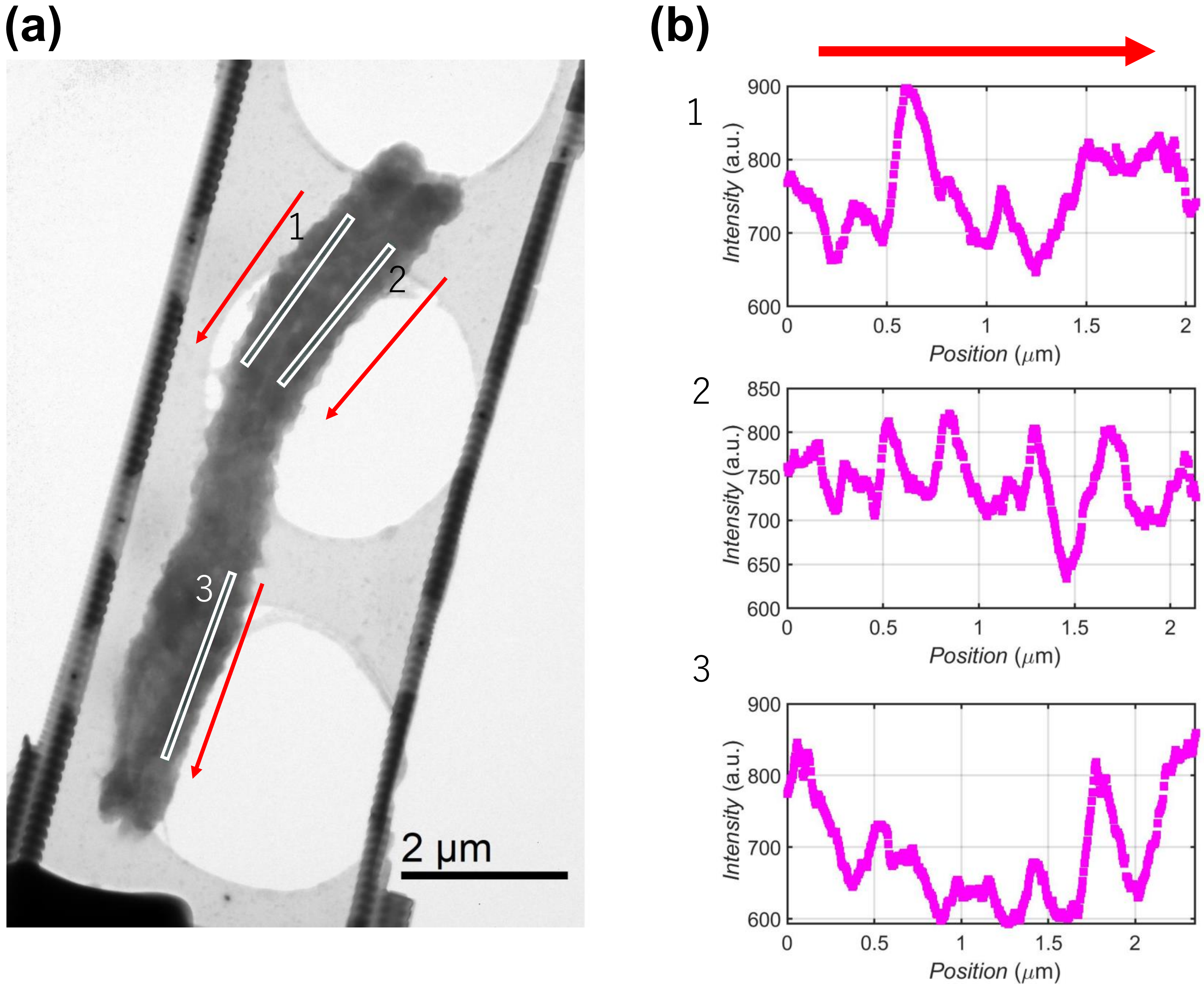
(a)
1
2
3
2 µm
(b)
1
900
800
700
600
Intensity (a.u.)
0
0.5
1
1.5
2
Position (µm)
2
850
800
750
700
650
600
Intensity (a.u.)
0
0.5
1
1.5
2
Position (µm)
3
900
800
700
600
Intensity (a.u.)
0
0.5
1
1.5
2
Position (µm)

Fig. 4